Single-Molecule Magnets

DOI: 10.1002/anie.201201478

Coexistence of Distinct Single-Ion and Exchange-Based Mechanisms for Blocking of Magnetization in a $Co^{II}_2Dy^{III}_2$ Single-Molecule Magnet**

Kartik Chandra Mondal, Alexander Sundt, Yanhua Lan, George E. Kostakis, Oliver Waldmann, Liviu Ungur, Liviu F. Chibotaru,* Christopher E. Anson, and Annie K. Powell**

In memory of Ian J. Hewitt

Research efforts in the quest for new single-molecule magnets (SMMs) have increasingly focused on systems either based on or else incorporating 4f ions.[1] For most pure 3d systems, and especially those containing the Mn^{III} ion such as the original Mn_{12}-Ac coordination cluster, spin reorientation is blocked when the ground state spin (S) combines with uniaxial magnetic anisotropy (D) to give an energy barrier to magnetic relaxation with the superexchange interactions between the metal centers leading to a molecular spin ground state and a molecular anisotropy.[2,3] The resultant exchange-based blocking of magnetization can be analyzed using a giant spin model.[4] In systems incorporating highly anisotropic 4f ions[1] it has become clear that magnetic interactions between 4f ions are weak and generally dipolar in nature. Here the single-ion spin and anisotropy become of greater relevance. For example, recent calculations on a Dy_2 SMM showed that the blocking mechanism largely arises from the individual Dy^{III} ions with exchange-based behavior only seen at very low temperatures.[5] In systems combining 3d and 4f ions the aim is to embed highly anisotropic 4f ions into an exchange-coupled molecular 3d system, since 3d–4f interactions can be intermediate in magnitude between 3d–3d and 4f–4f. However, analysis of the origins of the blocking mechanism in such systems is not straightforward and can generally only be achieved through detailed ab initio calculations, such as we recently reported for a Cr_4Dy_4 SMM.[6] We now present a SMM comprising two Co^{II} and two Dy^{III} ions for which we can demonstrate the novel situation of single-ion blocking of the Dy^{III} ions at higher temperatures with a crossover to molecular exchanged-based blocking at low temperatures.

Reaction of $Dy(NO_3)_3\cdot 6H_2O$, $Co(NO_3)_2\cdot 6H_2O$, H_2L and Et_3N in the molar ratio 1:1:2:4 in MeOH gives crystalline red powder which was recrystallized from THF giving pink crystals of $[Co_2Dy_2(L)_4(NO_3)_2(THF)_2]\cdot 4THF$ (**1**) in 75% yield. H_2L is the Schiff-base we previously described[7] resulting from condensation of *o*-vanillin and 2-aminophenol to give a "pocket ligand" capable of binding two different types of metal ion (see Figure S1 in the Supporting Information).

Compound **1** crystallizes in the triclinic space group $P\bar{1}$ with $Z = 1$. Within the core of the centrosymmetric complex, the metal ions are linked by four $(L)^{2-}$ ligands in the butterfly (or defect-dicubane) topology (Figure 1). One of the two crystallographically independent ligands chelates Dy(1) through its imine nitrogen and the two phenolate oxygens O(1) and O(3) (corresponding to pocket I, see Figure S1 in the Supporting Information). Co(1) and Co(1′) are linked

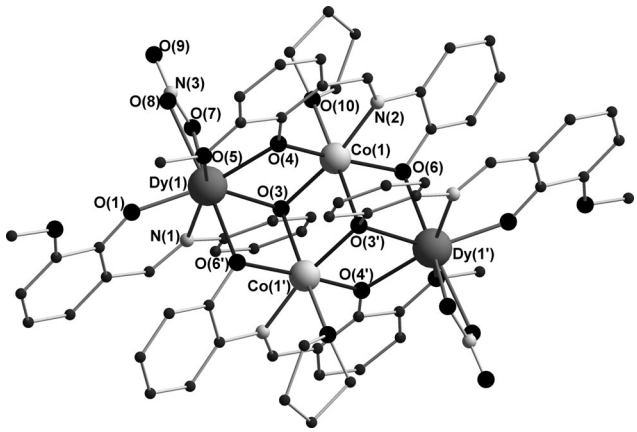

Figure 1. Molecular structure of the Co_2Dy_2 complex in **1**.

[*] Dr. K. C. Mondal, Dr. Y. Lan, Dr. C. E. Anson, Prof. Dr. A. K. Powell
Institute of Inorganic Chemistry, Karlsruhe Institute of Technology
Engesserstrasse 15, 76131 Karlsruhe (Germany)
E-mail: annie.powell@kit.edu
Dr. L. Ungur, Prof. Dr. L. F. Chibotaru
Division of Quantum and Physical Chemistry and
INPAC—Institute of Nanoscale Physics and Chemistry
Katholieke Universiteit Leuven
Celestijnenlaan 200F, 3001 Heverlee (Belgium)
E-mail: liviu.chibotaru@chem.kuleuven.be
Dr. K. C. Mondal, Dr. G. E. Kostakis, Prof. Dr. A. K. Powell
Institute of Nanotechnology, Karlsruhe Institute of Technology
76204 Karlsruhe (Germany)
A. Sundt, Prof. O. Waldmann
Physikalisches Institut, Universität Freiburg
Hermann-Herder-Strasse 3, 79104 Freiburg (Germany)

[**] Financial support by INPAC and Methusalem grants of the University of Leuven (L.U.), DFG-CFN (Y.L.), and DFG-TR-SFB-3MET (A.K.P.). We thank F. Axtmann for help in experiments. L.U. is a post-doc of the FWO-Vlaanderen (Flemisch Science Foundation).

Supporting information for this article is available on the WWW under http://dx.doi.org/10.1002/anie.201201478.

through a μ_3-OR-bridge from the phenolate O(3) which also connects to Dy(1) to form a Co_2Dy triangle. The other ligand chelates Co(1) through pocket I as well as the O(4) and O(5) donors of pocket II which also coordinate Dy(1) with the (amino)phenolate O(6) bridging to Dy(1′). The ligand and its inversion equivalent provide μ-OR bridges along the four outer edges of the Co_2Dy_2 rhombus with a chelating nitrate on Dy^{III} and the O(10) oxygen of THF Co^{II} completing the respective coordination spheres. Co(1) has a slightly distorted octahedral geometry with an O_5N donor set whilst the O_7N donor set about Dy(1) is close to pentagonal-bipyramidal geometry if we regard the chelating nitrate as a single donor (similar cone angle as for a chloride) on an axial site (Figure S2 in the Supporting Information). The complexes are surrounded by lattice THF molecules which prevent any intercomplex π–π stacking and the intermolecular Dy···Dy distances are over 10 Å. Full details of the structure are in the Supporting Information with selected bond lengths and angles in Table S2.

The magnetic data of **1** were collected on a powdered polycrystalline sample. The dc χT product under applied direct current (dc) magnetic fields ranging from 0.01 to 1 T in the temperature range of 1.8 to 300 K (Figure 2) show that

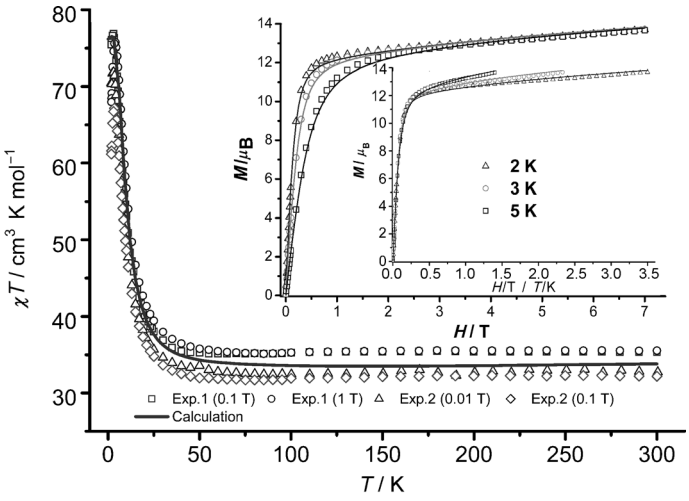

Figure 2. χT versus T at different applied dc fields. Inset: M versus H and M versus H/T plots at indicated temperatures. Experimental data: unfilled symbols; solid lines: ab initio calculated magnetism (see text for details).

with decreasing temperature, the χT product slightly decreases from 300 to 55 K, then sharply increases to 3 K before decreasing again down to 1.8 K. The behavior between 55 and 3 K suggests intramolecular ferromagnetic interactions dominate. The room-temperature χT value of about 35.3 $cm^3 K mol^{-1}$ per molecule is higher than the expected value of 32.1 $cm^3 K mol^{-1}$ (Co^{II}: $S = 3/2$, $g = 2$; and Dy^{III}: $S = 5/2$, $L = 5$, $^6H_{15/2}$, $g_J = 4/3$) consistent with the presence of ferromagnetic interactions with some contribution from the unquenched orbital contribution from the Co^{II} ions.[8] The field dependence of magnetization (Figure 2, inset) below 5 K abruptly increases below 0.5 T confirming the presence of ferromagnetic interactions in **1**. At higher field the magnetization curve follows a linear slope and reaches 15.2 μ_B without saturation even up to 7 T, suggesting the presence of low-lying excited states and/or magnetic anisotropy in **1**.[9,10]

The strong temperature and frequency dependences of the in-phase (χ') and out-of-phase (χ'') alternating current (ac) susceptibility signals under zero dc field (Figure 3 and Figures S4 and S5) are characteristic of SMM behavior. The

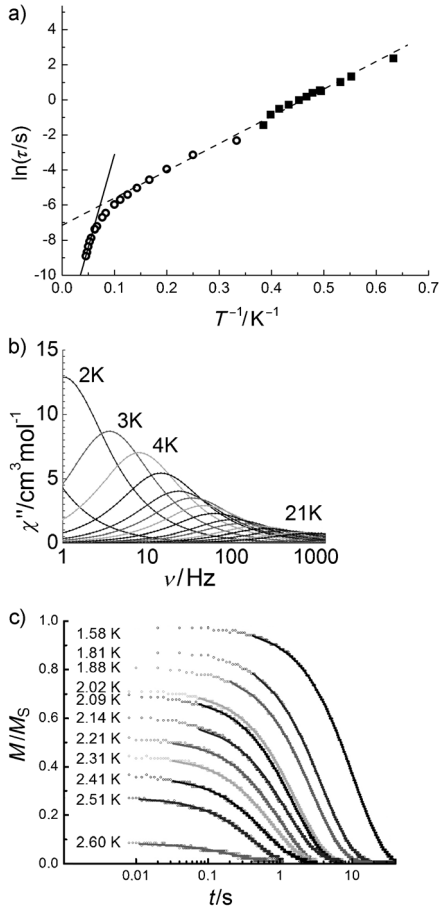

Figure 3. a) Logarithm of the relaxation time τ plotted as a function of $1/T$. Empty circles refer to the data extracted from the ac out-of-phase signal and full squares to those extracted from dc magnetic decay measurements. The lines represent Arrhenius fits to the data in the temperature range 1.6–8 K and 18–22 K, yielding $\Delta E_1 = 11.0\ cm^{-1}$, $\tau_1 = 7.7 \times 10^{-4}$ s, and $\Delta E_2 = 82.1\ cm^{-1}$, $\tau_2 = 6.2 \times 10^{-7}$ s, respectively. b) Frequency dependence of the ac out-of-phase susceptibility for $T = 2$ to 25 K. c) Dc magnetization decay curves for $T = 1.6$–2.6 K.

frequency dependence of the ac susceptibility was analyzed using the Debye model to extract the relaxation time τ, plotted as a function of $1/T$ in Figure 3a. There are two thermally activated regimes with $\Delta E_1 = 11.0\ cm^{-1}$ and $\tau_1 = 7.7 \times 10^{-4}$ s in the temperature range 1.6–8 K and $\Delta E_2 = 82.1\ cm^{-1}$ and $\tau_2 = 6.2 \times 10^{-7}$ s between 18 and 22 K. Notably, the regime of quantum tunneling of magnetization is still not achieved within the investigated temperature domain. A nearly symmetrical Cole–Cole (Argand) plot results between

5 and 21 K (Figure S5). Fitting the diagram at each temperature to the generalized Debye model leads to a parameter α ranging from 0.024 to 0.012 over the temperature range 8–15 K, while in the high-temperature regime above 18 K the parameter α is found to be always less than 0.009 (Figure S5, Table S3) indicating a very narrow distribution of relaxation times for each process.

To confirm the SMM behavior, hysteresis loops were recorded using a micro-Hall magnetometer for which a sufficient range of sweep rates is available[11] on a crystal well coated in Apiezon grease. Even if such a crystal fractures on cooling the grease prevents any movement of the fragments and the measurements correspond to those on aligned single crystallites. Hysteresis was clearly observed below 3 K at a sweep rate of 235 $mT\,s^{-1}$. The coercive fields of the hysteresis loops increase with decreasing temperature and increasing field sweep rates (Figure 4 and Figure S6). The loops display steplike features below 1.5 K, indicating that resonant quantum tunneling occurs below this temperature. Time decay measurements of the dc magnetization were performed in zero magnetic field on a single crystal of **1** in the temperature range 1.6 to 2.6 K (Figure 3c). The data could be fitted well using single-exponential time decay curves.

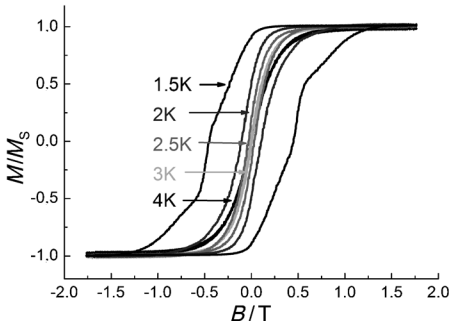

Figure 4. Temperature-dependent magnetic hysteresis loops of **1** below 4 K and a sweep rate of the external magnetic field of 235 $mT\,s^{-1}$.

Fragment ab initio calculations using the previously described MOLCAS program package[12] were performed on **1** (see also the Supporting Information).[6,13] The calculated lowest energy levels on the Co^{2+} and Dy^{3+} centers in **1** are given in Table 1 and the dashed lines in Figure 5 show the resulting orientation of the local anisotropy axes on Dy^{3+} ions with respect to the molecular frame in **1**.

The exchange interaction in **1** was calculated within the Lines model (see the Supporting Information for details).[14] Table 2 shows the spectrum of the lowest exchange levels. These levels are grouped into doublets split by an amount Δ_t because of the even number of electrons in **1**. Such Ising doublets are characterized by one single direction of magnetization Z, which varies according to the doublet and zero transversal magnetization ($g_X = g_Y = 0$). On the other hand, the inversion symmetry of the complex, according to which the anisotropy axes on the opposite ions in **1** are parallel to each other in addition to the predominant Ising interaction, makes some of the exchange doublets in Table 2 nonmagnetic ($g_Z = 0$).

Table 1: Energy (cm^{-1}) of the lowest Kramers doublets on individual magnetic centers in **1**. Only the states corresponding to the free ion ^4T term on Co^{2+} and to the multiplet $J = 15/2$ of the free ion Dy^{3+} are presented.

Dy	Co
0.0	0.0
192.6	109.1
307.7	1045.5
386.2	1276.2
430.9	1624.0
509.0	1750.8
565.8	
627.9	
main values of the g tensor of the lowest Kramers doublets	
$g_X = 0.005$	$g_X = 1.89$
$g_Y = 0.008$	$g_Y = 3.24$
$g_Z = 19.53$	$g_Z = 6.74$

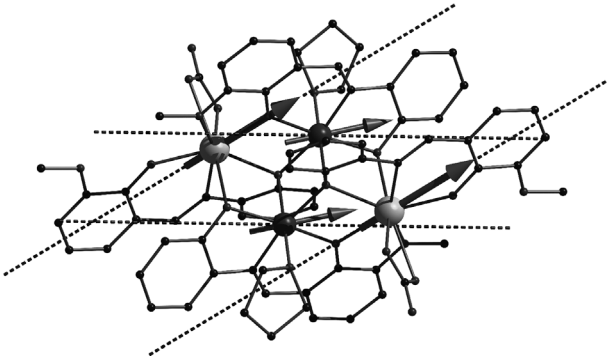

Figure 5. Main anisotropy axes (dashed lines) on Dy and Co ions and local magnetizations (arrows) in the ground state in **1**.

Table 2: Lowest exchange spectrum (cm^{-1}) arising from the exchange interaction of the lowest Kramers doublets on magnetic centers in **1**.

Energy	Δ_t	g_Z
0.0	1.7×10^{-6}	49.4
12.5	7.8×10^{-6}	0.0
13.4	5.9×10^{-6}	0.0
15.9	1.4×10^{-5}	39.5
17.9	8.4×10^{-7}	0.0
20.1	7.0×10^{-7}	39.7
20.5	1.4×10^{-7}	0.0
26.5	3.7×10^{-6}	31.8

This arises because for these doublet states, the magnetic moments on the two Dy^{III} and two Co^{II} ions point in opposite directions and completely compensate each other. In contrast, in the ground exchange doublet they are parallel to each other (Figure 5) resulting in a large magnetic moment $\mu_Z = 1/2\, g_Z \mu_B$, $g_Z = 24.7\ \mu_B$ (Table 2). As a result of the exchange interaction, local magnetizations on the Co^{II} ions make an angle of about 13.2° with the main anisotropy axis g_Z of the ground Kramers doublet, while on Dy^{III} this angle is only 0.3° (Figure 5). A comparison of measured and calculated magnetism is shown in Figure 2.

Table 2 shows that the ground exchange doublet is characterized by a relatively small tunneling gap, which

explains why quantum tunneling of magnetization is suppressed until very low temperatures are reached (Figure 3). The fourth exchange doublet has a tunneling gap of the order 10^{-5} cm^{-1}, which opens the channel for tunneling relaxation of magnetization through this state.[15] We can, therefore, associate the height of the barrier (11.0 cm^{-1}) to the relaxation regime at $T<18$ K (dashed line in Figure 3a) with this state.

On the other hand the Arrhenius regime of relaxation observed at $T>18$ K (solid line in Figure 3a) cannot be associated with the exchange states since the highest of these states (26 cm^{-1}, Table 2) lies much lower than the value of the extracted barrier (82 cm^{-1}), meaning that this regime must be associated with relaxation through excited Kramers doublets of individual metal ions, as previously inferred for some Dy complexes.[16] The condition for this relaxation regime to be observed in ac measurements is $\omega\tau_i \approx 1$,[17] where $\tau_i(T)$ is the intraionic relaxation time and ω is the frequency of the ac field. Table 1 tells us that the Dy^{III} ions are much more axial (g_X, $g_Y \ll g_Z$) than the Co^{II} ions and, therefore, should possess much longer relaxation times. Hence, for $\omega \leq 1000$ Hz the observed maximum of $\chi''(\omega)$ at $T>18$ K (Figure 3b and Figure S4) should be attributed to the intraionic relaxation through the Dy^{III} ion.[17] As additional confirmation of a very fast relaxation on the Co^{II} ions in **1**, the ac measurements made on the isostructural compound Co_2Y_2 show a zero out-of-phase signal. The calculated lowest excitation energy on the Dy^{III} sites (Table 1) is higher than the estimated height of the barrier for this regime, which probably results from the lack of sufficient temperature points being taken in the high-T region in Figure 3 as a result of instrumental limitations.[18]

The two relaxation regimes can also be seen in the temperature dependence of $\chi'(\omega)T$ for $\omega>1000$ Hz (Figure 6). The downturn of $\chi'T$ from the isothermal curve at 1500 Hz can be associated with quenching of intraionic relaxation mediated by Dy^{III} ions when $\omega\tau_{Dy}(T)$ becomes >1.[4] The $\chi'T$ value drops with approximately constant slope by a value roughly corresponding to the contribution of two Dy^{III} ions, this corresponding to the regime where the single ion contributions dominate. At lower temperatures, the further drop of $\chi'T$, but with a shallower slope (Figure 6) is where the presence of the Co^{II} ions becomes important and can be attributed to the exchange-blocked relaxation regime where the cooperative coupling of the 3d and 4f ions dominates.

Such a switch to the exchange-blocked relaxation regime at low temperatures has been inferred recently for Dy_2 complexes.[5] Here, however this can be unambiguously identified since for **1** (Figure 3) the two regimes on the ln(τ) versus 1/T curve can be observed thanks to the 10-times larger exchange splitting of the low-lying levels seen here compared with the Dy_2 complex. This is a direct result of the presence of the 3d ions and allows us to come to the important conclusion that the observation of two curves of different gradient, as seen in Figure 3, can be taken as the signature of mixed 3d–4f SMMs. A similar, but more dramatic, behavior is expected in mixed 4,5d–4f complexes, which in addition will possess larger exchange barriers than **1** because of more diffuse magnetic orbitals on the transition-metal ions and, therefore, should be regarded as most promising for the design of effective and efficient SMMs.

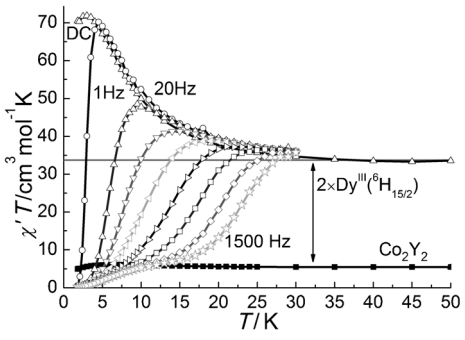

Figure 6. Temperature dependence of the DC susceptibility χ' times temperature T of **1** (△), the in-phase ac susceptibility χ' times T for the frequencies 1, 20, 50, 100, 200, 400, 800, and 1500 Hz from left to right (○ and empty star), and the measured χT value of Co_2Y_2 (■). Also shown (horizontal line) is the χT value as determined from the room-temperature Curie constant of Co_2Y_2 plus two times that of a free Dy^{III} ion.

Experimental Section

Crystallography: Structures solved and refined using SHELXTL 6.14.[19] **1**: $C_{80}H_{92}Co_2Dy_2N_6O_{24}$ (1964.46 g mol^{-1}), triclinic, $P\bar{1}$, $a=11.7308(9)$, $b=13.2206(11)$, $c=14.9021(12)$ Å, $\alpha=109.568(7)$, $\beta=93.391(6)$, $\gamma=113.742(6)°$, $V=1951.0(3)$ Å^3, $T=150(2)$ K, $Z=1$, $\rho_c=1.672$ g cm^{-3}, $F(000)=992$, μ(Mo-Kα)$=2.393$ mm^{-1}. 16703 reflections measured, 9316 unique ($R_{int}=0.0256$), refinement (510 parameters) to $wR_2=0.1060$, S$=0.997$ (all data), $R_1=0.0411$ (8192 data with $I>2\sigma(I)$), largest peak/hole 0.86/−2.46 e Å^{-3}. **2**: $C_{80}H_{92}Co_2N_6O_{24}Y_2$ (1817.28 g mol^{-1}), triclinic, $P\bar{1}$, $a=11.7437(12)$, $b=13.2227(13)$, $c=14.9685(14)$ Å, $\alpha=109.024(6)$, $\beta=93.149(8)$, $\gamma=113.694(7)°$, $V=1956.5(3)$ Å^3, $T=180(2)$ K, $Z=1$, $\rho_c=1.542$ g cm^{-3}, $F(000)=938$, μ(Mo-Kα)$=1.968$ mm^{-1}. 13449 reflections measured, 8261 unique ($R_{int}=0.0209$), refinement (510 parameters) to $wR_2=0.1006$, $S=0.972$ (all data), $R_1=0.0378$ (7037 data with $I>2\sigma(I)$), largest peak/hole 0.74/−0.55 e Å^{-3}. CCDC 853440, 853441 contain the supplementary crystallographic data for this paper. These data can be obtained free of charge from The Cambridge Crystallographic Data Centre via www.ccdc.cam.ac.uk/data_request/cif.

Received: February 23, 2012
Published online: June 12, 2012

Keywords: ab initio calculations · cobalt · high-energy barriers · lanthanides · single-molecule magnets

[1] R. Sessoli, A. K. Powell, *Coord. Chem. Rev.* **2009**, *253*, 2328–2341, and references therein.

[2] a) A. Caneschi, D. Gatteschi, R. Sessoli, A. L. Barra, L. C. Brunel, M. Guillot, *J. Am. Chem. Soc.* **1991**, *113*, 5873; b) L. Thomas, F. Lionti, R. Ballou, D. Gatteschi, R. Sessoli, B. Barabara, *Nature* **1996**, *383*, 145; c) J. R. Friedman, M. P. Sarachik, J. Tejada, R. Ziolo, *Phys. Rev. Lett.* **1996**, *76*, 3830; d) S. Hill, R. S. Edwards, N. Aliaga-Alcalde, G. Christou, *Science* **2003**, *302*, 1015.

[3] G. Aromí, E. K. Brechin, *Struct. Bonding (Berlin)* **2006**, *122*, 1, and references therein.

[4] D. Gatteschi, R. Sessoli, J. Villain, *Molecular nanomagnets*, Oxford University Press, Oxford, **2006**.
[5] Y.-N. Guo, G.-F. Xu, W. Wernsdorfer, L. Ungur, Y. Guo, J. Tang, H.-J. Zhang, L. F. Chibotaru, A. K. Powell, *J. Am. Chem. Soc.* **2011**, *133*, 11948.
[6] J. Rinck, G. Novitchi, W. van den Heuvel, L. Ungur, Y. Lan, W. Wernsdorfer, C. E. Anson, L. F. Chibotaru, A. K. Powell, *Angew. Chem.* **2010**, *122*, 7746; *Angew. Chem. Int. Ed.* **2010**, *49*, 7583.
[7] K. C. Mondal, G. E. Kostakis, Y. Lan, W. Wernsdorfer, C. E. Anson, A. K. Powell, *Inorg. Chem.* **2011**, *50*, 11604.
[8] a) X.-Q. Zhao, Y. Lan, B. Zhao, P. Cheng, C. E. Anson, A. K. Powell, *Dalton Trans.* **2010**, *39*, 4911; b) V. Chandrasekhar, B. M. Pandian, R. Azhakar, J. J. Vittal, R. Clérac, *Inorg. Chem.* **2007**, *46*, 5140; c) V. Chandrasekhar, B. M. Pandian, R. Azhakar, J. J. Vittal, R. Clérac, *Inorg. Chem.* **2009**, *48*, 1148; d) F. Chen, W. Lu, Y. Zhu, B. Wu, X. Zheng, *J. Coord. Chem.* **2009**, *62*, 808; e) H. Xiang, Y. Lan, H.-Y. Li, L. Jiang, T.-B. Lu, C. E. Anson, A. K. Powell, *Dalton Trans.* **2010**, *39*, 4737.
[9] J. D. Rinehart, K. R. Meihaus, J. R. Long, *J. Am. Chem. Soc.* **2010**, *132*, 7572.
[10] C. Benelli, D. Gatteschi, *Chem. Rev.* **2002**, *102*, 2369, and references therein.
[11] D. Schray, G. Abbas, Y. Lan, V. Mereacre, A. Sundt, J. Dreiser, O. Waldmann, G. E. Kostakis, C. E. Anson, A. K. Powell, *Angew. Chem.* **2010**, *122*, 5312; *Angew. Chem. Int. Ed.* **2010**, *49*, 5185.
[12] F. Aquilante, L. De Vico, N. Ferre, G. Ghigo, P. A. Malmqvist, P. Neogrady, T. B. Pedersen, M. Pitonak, M. Reiher, B. O. Roos, L. Serrano-Andres, M. Urban, V. Veryazov, R. Lindh, *J. Comput. Chem.* **2010**, *31*, 224.
[13] a) L. Ungur, W. Van den Heuvel, L. F. Chibotaru, *New J. Chem.* **2009**, *33*, 1224; b) L. F. Chibotaru, L. Ungur, A. Soncini, *Angew. Chem.* **2008**, *120*, 4194; *Angew. Chem. Int. Ed.* **2008**, *47*, 4126; c) F.-S. Guo, J.-L. Liu, J.-D. Leng, Z.-S. Meng, Z.-J. Lin, M.-L. Tong, S. Gao, L. Ungur, L. F. Chibotaru, *Chem. Eur. J.* **2011**, *17*, 2458.
[14] L. F. Chibotaru, L.Ungur, Computer program POLY_ANISO, University of Leuven, **2006**.
[15] In a $Co^{II}_3Co^{III}_4$ wheel the lack of SMM behavior was explained by the existence of tunneling gap of 3×10^{-5} cm^{-1} in the ground exchange doublet in L. F. Chibotaru, L. Ungur, C. Aronica, H. Elmoll, G. Pilet, D. Luneau, *J. Am. Chem. Soc.* **2008**, *130*, 12445.
[16] P. H. Lin, T. J. Burchell, L. Ungur, L. F. Chibotaru, W. Wernsdorfer, M. Murugesu, *Angew. Chem.* **2009**, *121*, 9653; *Angew. Chem. Int. Ed.* **2009**, *48*, 9489.
[17] A counterexample is the complex $Dy^{III}_4Cr^{III}_4$ where the Dy^{III} ions were found to be nonaxial ($g_X=1.7$, $g_Y=5.8$, $g_Z=14.4$), and accordingly, no intraionic relaxation was detected in ac susceptibility measurements, see ref. [6]).
[18] A good agreement of calculated and measured magnetic properties (Figure 2) rules out the possibility of a large deviation of the energy of the first excited Kramers doublet on Dy from the value in Table 1.
[19] G. M. Sheldrick, SHELXTL 6.14, Bruker AXS Inc., 6300 Enterprise Lane, Madison, WI 53719-1173, USA **2003**.

